Interneurons secrete prosaposin, a neurotrophic factor, to attenuate kainic acid-induced neurotoxicity

Hiroaki Nabeka [a],[*],[1], Shouichiro Saito [b],[*],[1], Xuan Li [a], Tetsuya Shimokawa [a], Md. Sakirul Islam Khan [a], Kimiko Yamamiya [a], Soichiro Kawabe [c], Takuya Doihara [a], Fumihiko Hamada [d], Naoto Kobayashi [e], Seiji Matsuda [a]

[a] Department of Anatomy and Embryology, Ehime University Graduate School of Medicine, Toon, Ehime, Japan
[b] Laboratory of Veterinary Anatomy, Faculty of Applied Biological Sciences, Gifu University, Yanagido, Gifu, Japan
[c] Fukui Prefectural Dinosaur Museum, Fukui, Japan
[d] Department of Human Anatomy, Oita University Fuculty of Medicine, Yufu, Oita, Japan
[e] Medical Education Center, Ehime University Graduate School of Medicine, Toon, Ehime, Japan

ARTICLE INFO

ABSTRACT

Prosaposin (PS) is a secretory neurotrophic factor, as well as a regulator of lysosomal enzymes. We previously reported the up-regulation of PS and the possibility of its axonal transport by GABAergic interneurons after exocitotoxicity induced by kainic acid (KA), a glutamate analog. In the present study, we performed double immunostaining with PS and three calcium binding protein markers: parvalbumin (PV), calbindin, and calretinin, for the subpopulation of GABAergic interneurons, and clarified that the increased PS around the hippocampal pyramidal neurons after KA injection existed mainly in the axons of PV positive interneurons. Electron microscopy revealed PS containing vesicles in the PV positive axon. Double immunostaining with PS and secretogranin or synapsin suggested that PS is secreted with secretogranin from synapses. Based on the results from in situ hybridization with two alternative splicing forms of PS mRNA, the increase of PS in the interneurons was due to the increase of PS + 0 (mRNA without 9-base insertion) as in the choroid plexus, but not PS + 9 (mRNA with 9-base insertion). These results were similar to those from the choroid plexus, which secretes an intact form PS + 0 to the cerebrospinal fluid. Neurons, especially PV positive GABAergic interneurons, produce and secrete the intact form of PS around hippocampal pyramidal neurons to protect them against KA neurotoxicity.

1. Introduction

Secretory neurotrophic factors including brain-derived neurotrophic factor (BDNF), nerve growth factor (NGF), neurotrophin 3 or 4/5 (NT-3 or NT-4/5) promote neuronal survival. Unlike other growth factors, which are secreted via a constitutive pathway, BDNF is sorted into a regulated pathway with sortilin in response to neuronal activity (Lou et al., 2005; Evans et al., 2011).

Prosaposin (PS), a neurotrophic factor (Sano et al., 1994; Kotani et al., 1996a, 1996b; Tsuboi et al., 1998; Gao et al., 2013a, 2016), is also secreted by a mechanism for regulated secretion with sortilin (Yuan and Morales, 2011). Previously, we have reported the

possible PS secretion from the GABAergic interneurons via tau-positive axons around the hippocampal pyramidal neurons after kainic acid injection (Nabeka et al., 2014). PS is originally reported to be the precursor protein of four small lysosomal glycoproteins, saposins A, B, C, and D (Sano et al., 1988; O'Brien et al., 1988; O'Brien and Kishimoto, 1991; Kishimoto et al., 1992). Both saposins and PS are widely expressed in various tissues, although the brain, skeletal muscle and heart cells predominantly contain unprocessed PS rather than saposins (Sano et al., 1989, 1992; Kondoh et al., 1991, 1993; Hosoda et al., 2007; Terashita et al., 2007). In addition, unprocessed PS is found in various secretory fluids, such as seminal plasma, bile, pancreatic juice, human breast milk and cerebrospinal fluid (Hineno et al., 1991; Hiraiwa et al., 1992), and PS mRNA is strongly expressed in the choroid plexus (Saito et al., 2014).

Kainic acid (KA), a glutamate analogue, is a powerful neurotoxic agent (Olney and de Gubareff, 1978) that stimulates excitatory neurotransmitter release (Ferkany et al., 1982). Systemic KA injection induces neuronal degeneration in certain neuronal areas, includ-

* Corresponding authors.
E-mail addresses: nabeka@m.ehime-u.ac.jp (H. Nabeka), shouichi@gifu-u.ac.jp (S. Saito).
[1] Equal contribution. HN mainly contributes to immunohistochemistry, SS to in situ hybridization.

ing the hippocampus (Schwob et al., 1980; Nadler and Cuthbertson, 1980; Nadler et al., 1981; Heggli et al., 1981; Lothman and Collins, 1981; Nabeka et al., 2015). Hippocampal CA3 neurons are selectively vulnerable to KA, due to high levels of KA receptors in this region (Malva et al., 1998). KA can bind to the AMPA/KA receptors, and activation of its receptor has been shown to elicit a number of cellular events, including the increase in intracellular Ca2+, production of reactive oxygen species, and other biochemical events leading to neuronal cell death (see the review of Wang et al., 2005). This nature of neuronal degeneration caused by systemic KA injection resembles some forms of ischemia (Coyle, 1987) or epilepsy (Lévesque and Avoli, 2013). In recent years, neurodegeneration caused by systemic KA injection has been used to investigate mechanisms of the excitotoxic events (Sun and Chen, 1998; Dawson et al., 1995), and we also used KA to define the mechanisms of neurodegeneration and neuroprotection with PS (Nabeka et al., 2014, 2015).

Although the PS receptors have been defined as GPR37 and GPR37L1, orphan G protein- coupled receptors (Meyer et al., 2013), the movement of intrinsic PS in injured, as well as normal, nervous tissue remains unclear. We have shown that intrinsic PS and its mRNA increase in the facial nerve nucleus after nerve transection (Unuma et al., 2005; Chen et al., 2008) and decrease in the brain of mdx mice (Gao et al., 2013b), indicating its pivotal role in the survival of neurons and muscles.

In the previous study, we have shown the increase of PS immunoreactivity and its mRNA expression in the hippocampal and cortical neurons on day 3 after KA injection, and high PS levels were maintained even after 3 weeks. The increase in PS, but not saposins, suggested that the increase in PS-like immunoreactivity after KA injection was not due to an increase in PS for lysosomal enzymes after neuronal damage, but rather in PS for a neurotrophic factor to improve neuronal survival (Nabeka et al., 2014, 2015). The same study indicated that inhibitory interneurons as well as stimulated hippocampal pyramidal and cortical neurons synthesize PS for neuronal survival, and the choroid plexus is highly activated to synthesize PS, which may prevent neurons from excitotoxic neuronal damage (Nabeka et al., 2014).

In the present study, we aimed to clarify how PS act as a neurotrophic factor against exocitotoxic stimulation after systemic KA injection, for example which type of interneurons synthesize and

transport PS, and whether up-regulated PS is secretion type or intracellular type.

2. Materials And Methods

2.1. Animals

Ten-week-old male Wistar rats (320–350 g, total number = 28) were used in this study. All animals were provided by CLEA-Japan (Kyoto) and housed at a constant temperature (22 °C) under a 12:12-h light: dark cycle and given food and water *ad libitum*. This study was carried out in strict accordance with the recommendations of the Guidelines of the Animal Care Committee of Ehime University. The protocol was approved by the Animal Care Committee of Ehime University (Permit Number: 05A261) All animal experimentation have been conducted in accordance with the Society's Policies on the Use of Animals and Humans in Research. All surgery was performed under chloral hydrate (10 mg/kg) anesthesia, and all efforts were made to minimize suffering.

2.2. Antibodies

Anti-PS IgG (0.1 μg/mL) was prepared by Medical and Biological Laboratories (Nakaku, Nagoya, Japan) (Shimokawa et al., 2013). From the amino acid sequence of rat PS (M19936; Collard et al., 1988), a synthetic oligopeptide corresponding to the proteolytic portion of PS (409- PKEPAPPKQPEEPKQSALRAHVPPQK-434), which did not encode saposins, was used to generate a rabbit polyclonal antibody against rat PS. So, this anti-PS IgG reacts with PS but not any of four saposins (Nabeka et al., 2014).

To determine which type of interneurons synthesized and secreted PS, we used immunofluorescence method with the combination of rabbit anti-PS IgG and mouse anti-GAD67 (gulitamic acid decarboxylase 67, 1:500, Millipore, Temecula, CA, USA), mouse anti-PV (parvalbumin, 1:500, Sigma, St. louis, MO, USA), mouse anti-CB, or mouse anti-CR (calbindin, 1:500, calretinin, 1:500, SWANT, Bellinzona, Switzerland) as the primary antibodies (Figs. 1–6). As the second antibodies, we used Alexa Fluor 546 goat anti-rabbit IgG (H + L) (1:1000; Invitrogen, CA, USA) or Alexa
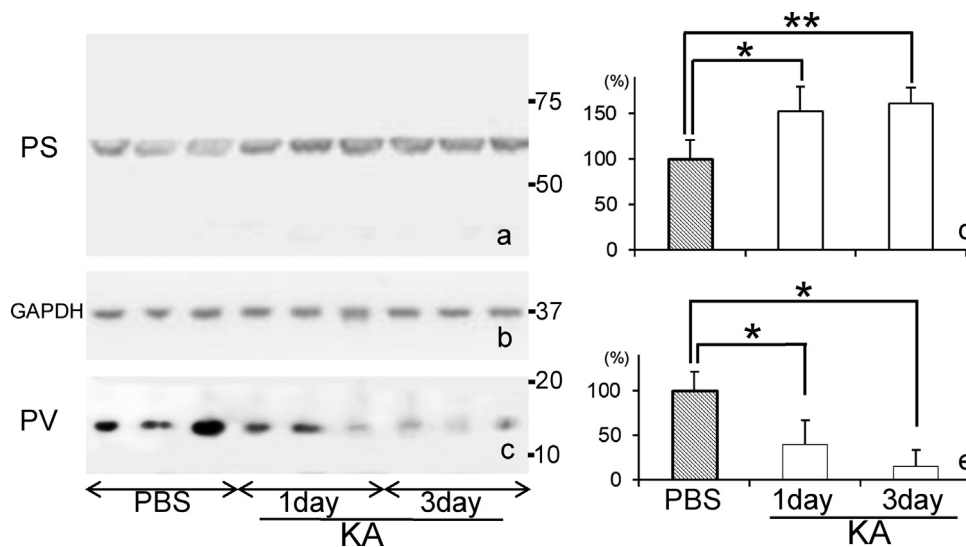

Fig. 1. a–d: Crude hippocampal extracts from normal control and from animals 1or 3 days after kainic acid (KA) injection were examined using anti-PS, GAPDH, PV antibodies. When stained with anti-PS (a), the single band observed at ∼ 69 kDa, which likely corresponded to PS, significantly increased in intensity after KA treatment (d). When stained with anti-PV (c), the single band observed at ∼ 12 kDa, which likely corresponded to PV, significantly decreased in intensity after KA treatment (e). The intensities of the protein bands were quantified using the NIH Image software (b, d), and PS and PV protein levels were expressed as % of vehicle (mean ± SD) normalized relative to GAPDH protein level. (*P < 0.05, **P < 0.01).
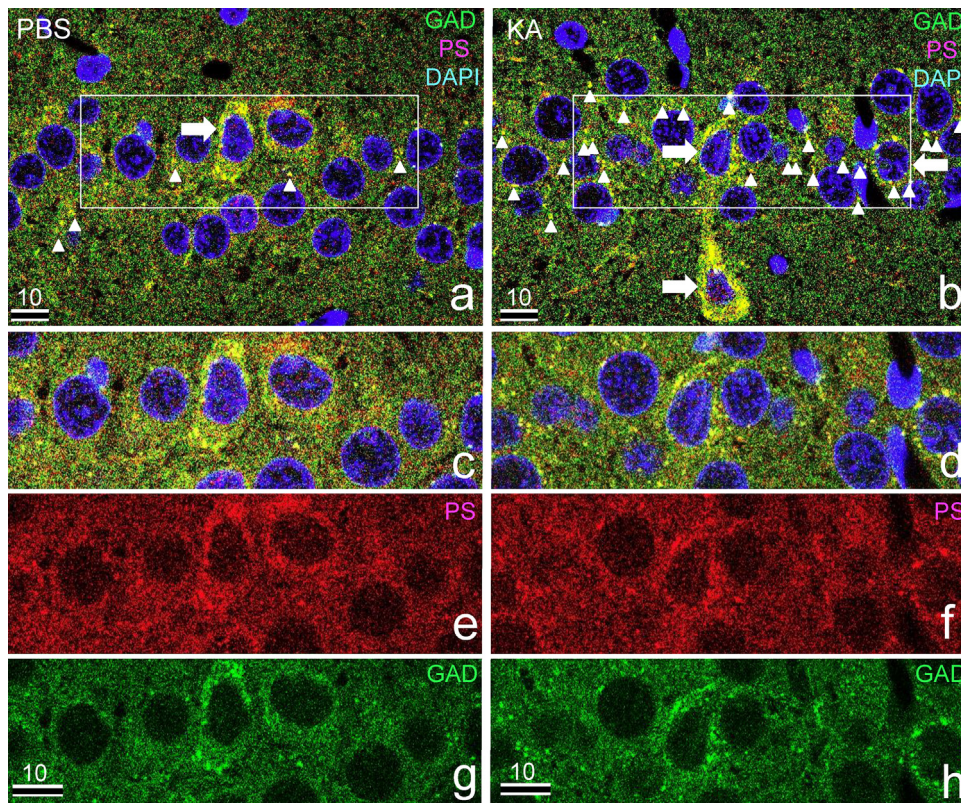
Fig. 2. Immunofluorescence light micrographs of the hippocampal CA1 neurons stained with anti-PS IgG, anti-GAD, and DAPI showing the PS-IR 3 days after PBS (a) or 5 mg/kg KA (b) injection. The cell body and axon terminals of GABAergic interneurons in the CA1 region were stained green with an anti-GAD antibody (a, b). The arrows indicate interneurons with slender nuclei and very intense immunoreactivity both of PS and GAD in the cytoplasm. Note that the GAD-PS double positive axon terminals are observed around almost all CA1 neurons after KA injection (b), but only some ones (arrowheads) are observed in the CA1 after PBS injection (a). Nuclei are stained with DAPI (blue), PS is shown red, and GAD is shown green. The numbers on the bar indicate μm.

Fluor 488 goat anti-mouse IgG (H + L) (1:1000; Invitrogen, CA, USA) and DAPI.

To detect PS in the PV positive-axon terminals of interneurons, anti-sposin D antiserum was used for immuno-electron microscopy (Fig. 6), because the above-mentioned anti-PS IgG dose not react with PS and only this anti-sposin D antiserum is usable and this antiserum was proven to show specific reaction to PS in the central nervous system (Hosoda et al., 2007).

To detect axonal transport of PS, we used immunofluorescence method with the combination of Alexa fluor 594 conjugated rabbit anti-PS IgG and FITC conjugated rabbit anti-secretogranin II (Bioss Inc. Mass, USA) (Fig. 7). Immunofluorescence method with the combination of rabbit anti-PS IgG and mouse anti-synapsin IIa (BD Biosciences, USA) was also used (Fig. 8).

2.3. KA injection

Rats (n = 6 per group) were anesthetized with an intraperitoneal injection of diethylether and clonazepam (0.2 mg/kg) as an anticonvulsant. After 10 min, the rats were anesthetized again with diethylether, and KA dissolved in normal saline was injected subcutaneously (5 mg/kg). After KA injection, the animals were housed at a constant temperature (22 °C), as the effects of KA depend, at least in part, on body temperature (Nabeka et al. 2014). Under these conditions, no animal experienced status epilepticus, even with KA, and no clear damage was observed at the ordinal light-microscopic level (Nabeka et al., 2014). Rats younger than 9 weeks that were injected with 5 mg/kg KA sometimes suffered some neuronal damage in the hippocampus, similar to observations in

10-week-old rats when injected with 8 mg/kg KA (Nabeka et al., 2014).

2.4. Analysis of PS, GAD, PV, CR, CB after KA injection using Western blot

The rats were anesthetized and injected with clonazepam (0.2 mg/kg), followed by 5 mg/kg KA as mentioned above. Three days after KA or PBS injection, the hippocampi of the rats (n = 6 per group) were dissected and homogenized in ice-cold 50 mM Tris-HCl (pH 6.8) buffer containing 0.1 M glycerol, 50 mM sodium dodecyl sulfate (SDS) and 4% protease inhibitor cocktail (Roche Diagnostics, Minatoku, Tokyo, Japan). The total protein extract was centrifuged at $12,000 \times g$ for 15 min at 4 °C, and the separated pellet was suspended in buffer in an equal volume as that of the supernatant. The solubilized proteins (50 μg) were separated by SDS-polyacrylamide gel electrophoresis (PAGE) on 10% polyacrylamide gels and transferred to a polyvinylidene difluoride membrane. The membrane was incubated with 5% BSA in TBS buffer (20 mM Tris-HCl, pH 7.4; 0.15 M NaCl) for 1 h at room temperature and then incubated with anti-saposin D serum (0.05 μg/mL) and anti-PS IgG (0.1 μg/mL) overnight at 4 °C. The membrane was then washed with TBS-T buffer (20 mM Tris-HCl, pH 7.4, 0.15 M NaCl, 1% Tween 20) and incubated with peroxidase-labeled anti-rabbit IgG (0.6 μg/mL; Dako, Glostrup, Denmark) for 1 h at room temperature, followed by treatment with the detection solution for enhanced chemiluminescence (ImmunoStar; Wako, Osaka, Japan). The immunoreactive protein bands were visualized using an LAS-4000 luminescence image analyzer (GE Healthcare Japan, Japan).
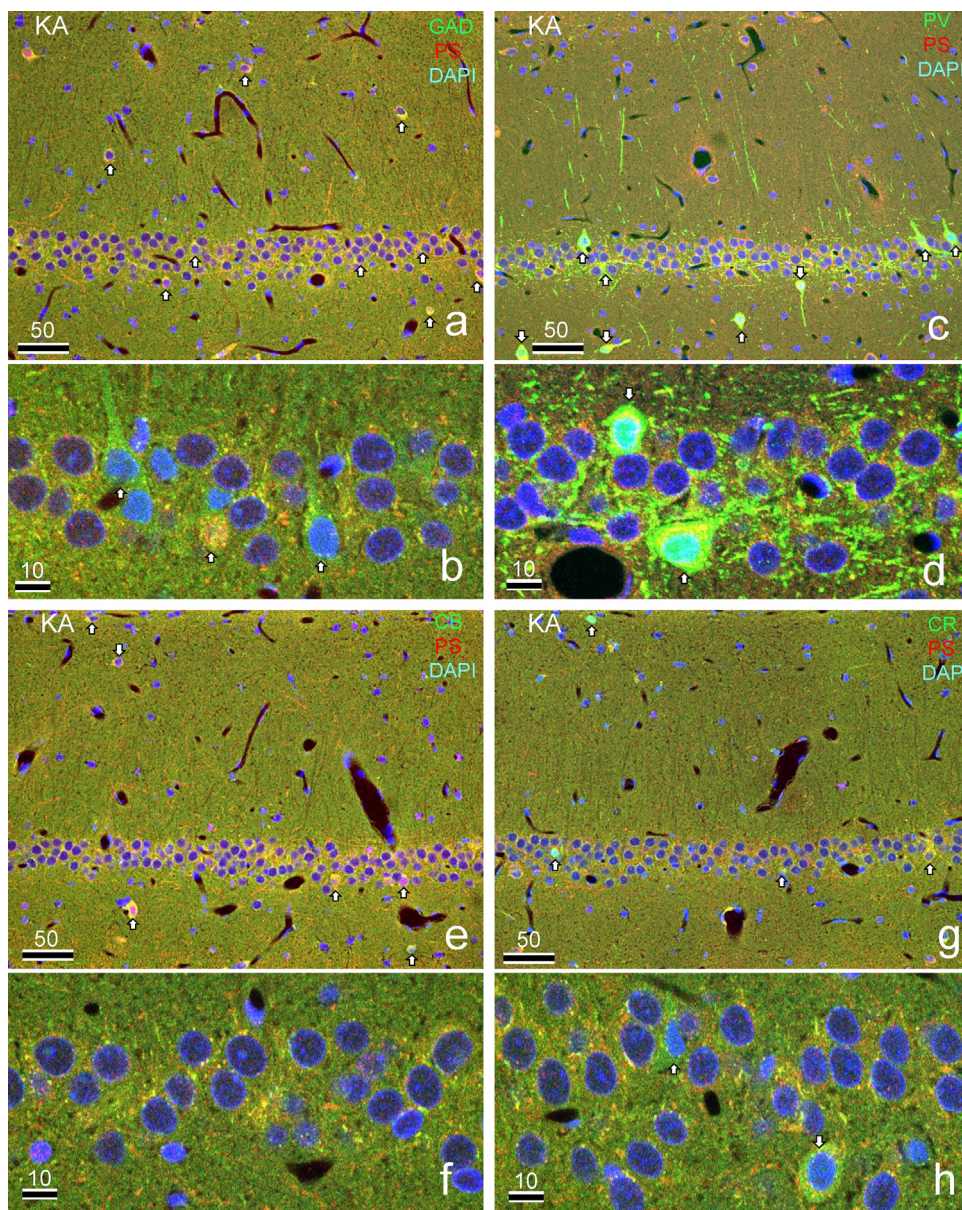
Fig. 3. Double immunofluorescence light micrographs of the rat hippocampal CA1 region 3 days after KA injection, stained with the antibody to PS and antibodies to GAD (a, b), PV (c, d), CB (e, f) or CR (g, h). Figures b, d, f and h are shown at a higher magnification of the CA1 pyramidal layers. PS are stained with anti-PS (red), cell bodies (indicated with arrows), axons and axon terminals of inhibitory neurons were stained with anti-GAD, PV, CB or CR (green), nuclei are stained with DAPI (blue), and merged. Note many putative axon terminals with strong PV −IR around the pyramidal neurons (d). The numbers on the bar indicate μm.

2.5. Immunostaining of PS and GAD, PV, CR, CB

Three days after KA or PBS injection, each animal was anesthetized by intraperitoneal injection of chloral hydrate (10 mg/kg) and perfused transcardially, first with 50-mL saline and then with 300-mL 4% paraformaldehyde in 0.1 M phosphate buffer. The brains were removed, cut into small pieces and post-fixed in the same solution for 4 h, and then embedded in paraffin using conventional methods, sectioned and deparaffinized. Following a brief rinse in PBS, the sections were exposed for 2 h to blocking solution containing 5% normal swine serum (NSS), 5% bovine serum albumin (BSA) and 0.25% carrageenan in PBS. The sections were processed for immunofluorescence with anti-PS antibody and anti-GAD, PV, CR, CB as the primary antibody at a 1:1,000 dilution.

After washing with PBS, the sections were treated for 1 h at room temperature with Cy3-conjugated goat anti-rabbit IgG (1:500; Rockland, Gilbertsville, PA, USA) for detection of PS. Some sections

were stained with rabbit anti-PS IgG and anti-GAD67 monoclonal antibody for GABA neurons, then treated with Cy3-conjugated goat anti-rabbit IgG (1:500; Rockland, Gilbertsville, PA, USA), Alexa Fluor 488 goat anti-mouse IgG (H + L) (1:1000; Life Technologies, Carlsbad, CA, USA) and DAPI. The sections were then washed with PBS, mounted in Mowiol (Calbiochem, San Diego, CA, USA) and examined using a Nikon A1 confocal microscope (Nikon, Tokyo, Japan) equipped with a 60 × objective lens (Nikon) (Fig. 2–5). The relative intensity of PS-IR signals in the hippocampal CA3 region was examined using computer-assisted image analysis as described below (Fig. 5).

2.6. Immunoelectron microscopy of PS and PV

Using the same anesthesia described above, the animals (n = 2 per group) were perfused transcardially with saline followed by 300 ml of 4% paraformaldehyde and 0.1% glutaraldehyde in 0.1 M

phosphate buffer. The tissues were cut into thick sections at 50 μm; cryoprotected with 10, 20, and 30% glycerol in phosphate buffer; and quick-frozen in anhydrous ethanol precooled with dry ice. The centrifuge tubes containing the above sections in the 0.5% uranyl acetate solution precooled with dry ice were covered with more than 5 kg of conventional cooling materials in an adiabatic box precooled with dry ice, and the box was kept at −80 °C for 24 h. The box was then moved to a freezer and kept at −30 °C for 24 h. The thick sections were rinsed with anhydrous ethanol three times at −30 °C; immersed in 30, 60, and 100% LR-White at −30 °C for 1 hr, then kept for 1 h at 4 °C, and polymerized at 55 °C for 10 hr. Ultrathin sections were made with a diamond knife and were mounted on nickel grids and incubated in blocking solution containing 5% BSA, 10% NSS, 0.1% Triton X-100, and 0.1% sodium azide in PBS for 2 h. The sections were incubated in the blocking solution containing the rabbit anti-saposin D serum at dilution of 1:50 and the mouse

anti-PV IgG at dilution of 1:50 at 4 °C overnight. After three rinses with the blocking solution, the section was incubated in the blocking solution containing two gold-conjugated Fab fragments (15 nm gold anti-rabbit and 5 nm gold anti-mouse) for 3 h. The section was rinsed with PBS, fixed in 1% glutaraldehyde in PBS for 10 min, rinsed with distilled water, double stained with uranyl acetate and lead citrate, and examined under a transmission electron microscope (H800; Hitachi, Tokyo, Japan).

2.7. Analysis of PS mRNA after KA injection using in situ hybridization

The probes for hybridization used in this study are listed in Table 1. The rats were anesthetized and injected with clonazepam (0.2 mg/kg) followed by 5 mg/kg KA as described above. Three days after KA injection, the rats (n = 6 per group) were decapi-
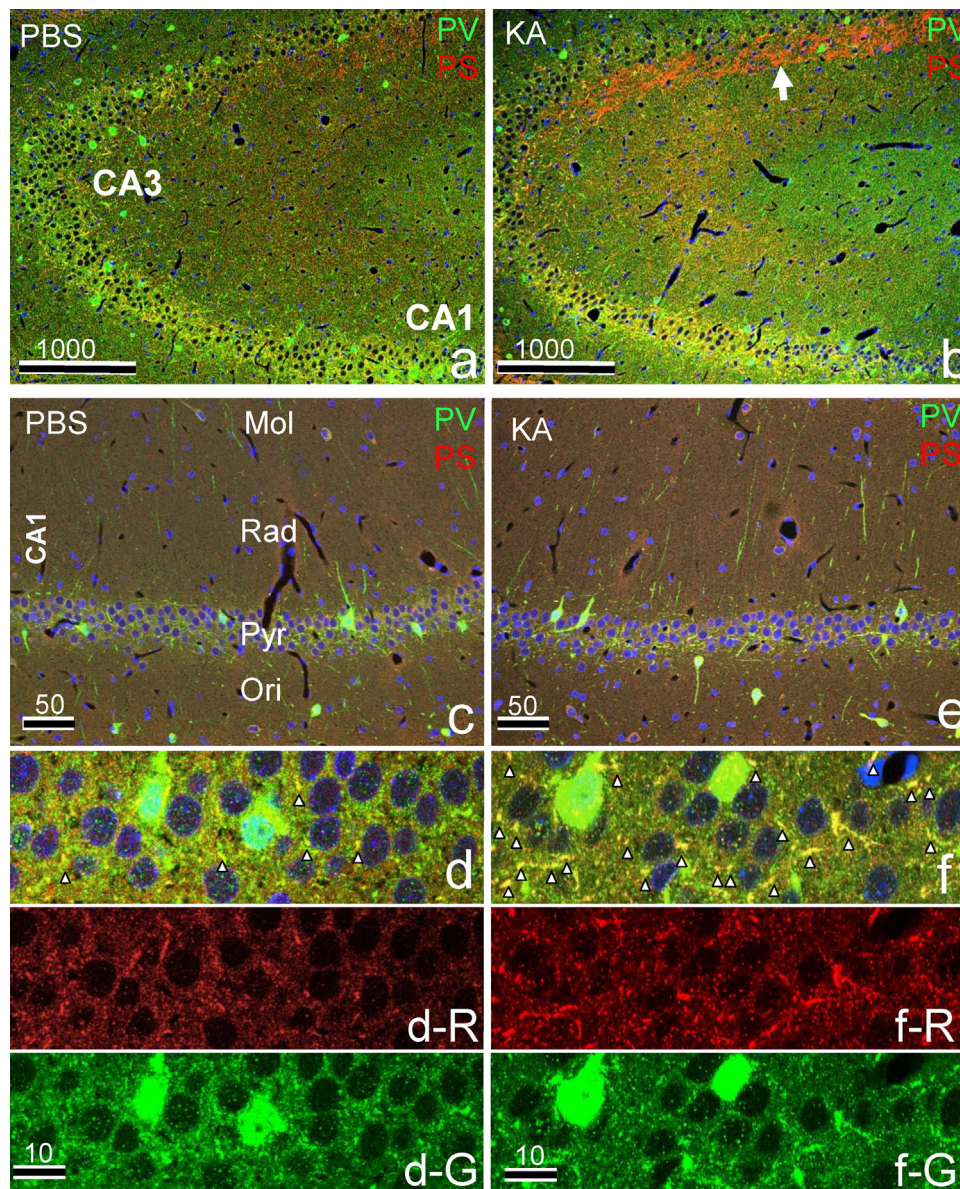

Fig. 4. Immunofluorescence light micrographs of the hippocampus (a and b), CA1 (c–f) and CA3 (g–j) regions, and dentate gyrus (DG) (k and l) of rats 3 days after PBS injection (left column) or KA injection (right column) are shown. The sections were stained with anti-PS, anti-PV, and DAPI. In the overall images of the hippocampus (a and b), note the increase in PS, especially in the pyramidal neurons and CA3 mossy terminals (arrow), and the decrease in PV-positive neurons. A higher magnification of the pyramidal layers of CA1 (d and f) or CA3 (h and j) is shown. The nuclei are stained with DAPI (blue), PS is stained with anti-PS (red), and the cell bodies, axons, and axon terminals are stained with anti-PV (green) and merged. Arrowheads indicate the axon terminals, which are double-stained with PS and PV (yellow). Mol: st. moleculare, Rad: st. radiatum, Pyr: st. pyramidale, Ori: st. orience, L-Mol: st. lacunosum-moleculare, Luc: st. lucidum, Gran: st. granulare. The numbers on the bar indicate μm.
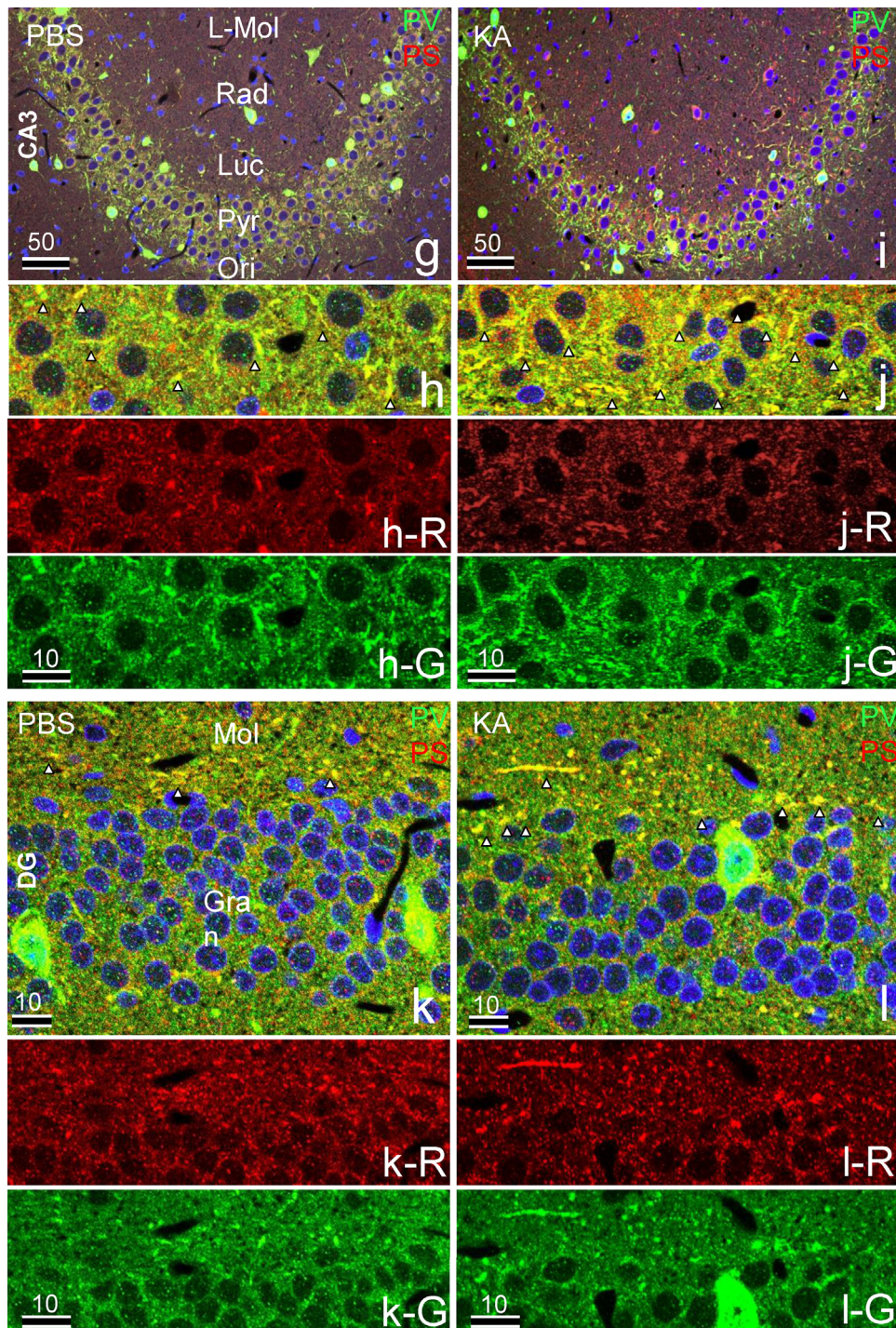
Fig. 4. (*Continued*)

Table 1
Probes for hybridization.

Probe name	Target	Sequence
PS-AS1	Pro + 0, Pro + 9	5′-TTCATTACCCTAGACCCACAAGTAGGCGACTTCTGC-3′
PS-AS3	Pro + 9	5′-CTTGGGTTGCTGATCCTGCATGTGCATCATCATCTG-3′
PS-AS4	Pro + 0	5′-TTCCTTGGGTTGCATGTGCATCATCATCTGGACGGC-3′
PS-S1	Complementary to PS-AS1	5′-GCAGAAGTCGCCTACTTGTGGGTCTAGGGTAATAGAA-3′

tated, the forebrains were frozen on dry ice and cut into 20-μm frontal sections using a cryostat. *In situ* hybridization to detect PS mRNA was performed as described previously (Unuma et al., 2005; Sato and Tohyama, 1998; Li et al., 2013). Briefly, Three anti-sense 36-mer oligonucleotide probes (PS-AS1, PS-AS3 and PS-AS4) and one sense probe (PS-S1) were synthesized (Table 1) com-
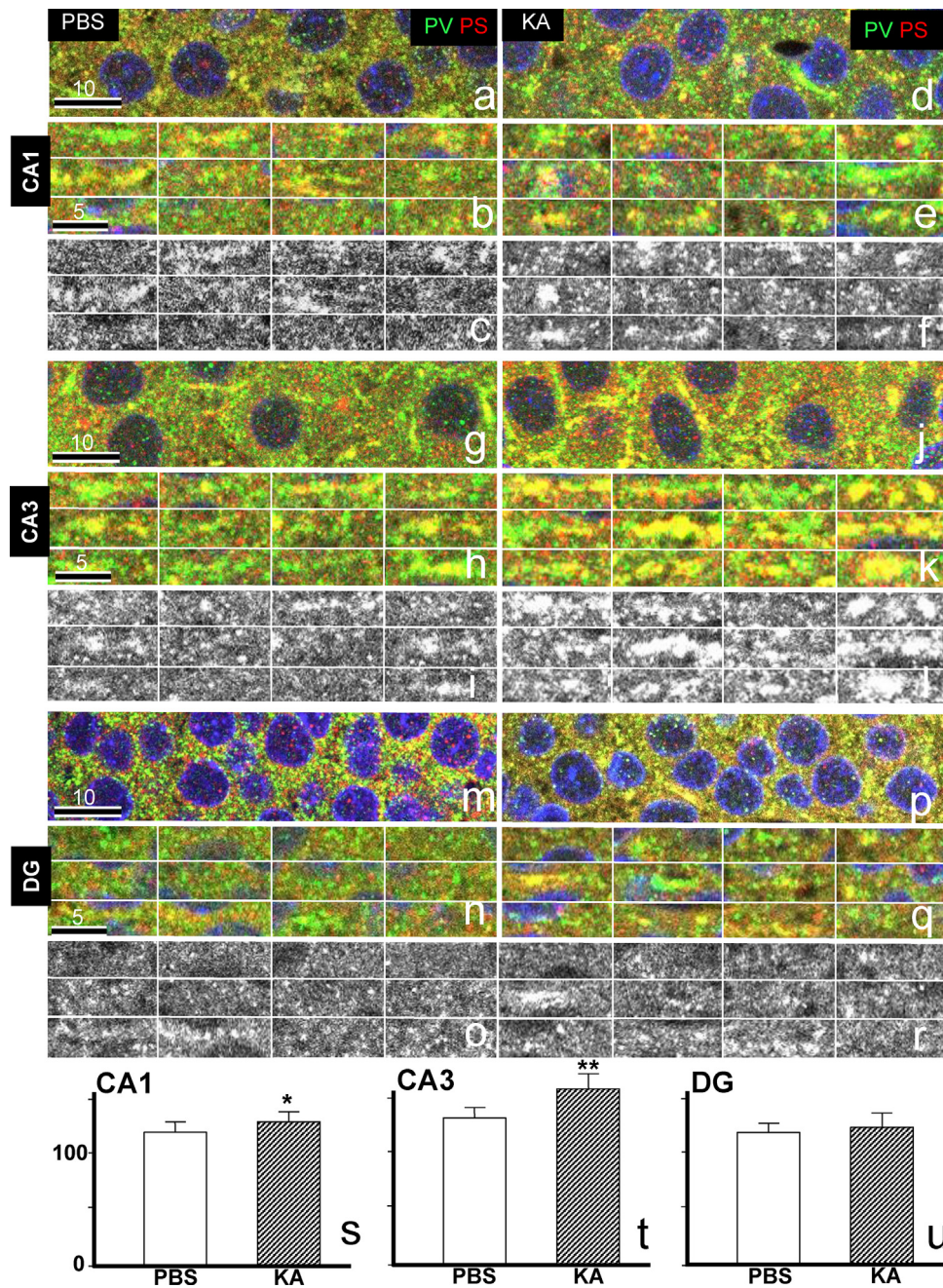
Fig. 5. Immunofluorescence light micrographs of PV-positive axons in the CA1, CA3 and DG regions of animals 3 days after PBS injection (left column) or KA injection (right column) stained with anti-PS, anti-PV and DAPI. Panels b, e, h, k, n and q are double positive axons intensely stained with anti-PS and anti-PV. Panels c, f, i, l, o and r are black-and-white images of the PS-IR (red) shown in b, e, h, k, n and q respectively, for the NIH Image analysis. Note that the PS-IR granules in the PV-positive axons in the KA-injected animals (l) are larger than those in the PBS injected ones (i). The ratio of PS-IR was significantly higher after KA injection compared with controls with PBS injection in CA1 ($^*p < 0.05$) and CA3 ($p^{**} < 0.01$). The numbers on the bar indicate μm.

mercially by Operon Biotechnologies (Tokyo, Japan). PS-AS3 and PS-AS4 are complementary to bases 834–869 of NM‗001190236 and bases 828–863 of NM‗013013, respectively. PS-AS1 is complementary to bases 1704–1739 in the 3′-untranslated region of prosaposin cDNA (M19936) and detects both Pro+0 mRNA and Pro+9 mRNA. The sense probe PS-S1, which is complementary to PS- AS1, was used as a control. The specificities of these 36-mer oligonucleotide probes have been demonstrated by dot-blot hybridization in the previous study (Saito et al., 2013). The frozen sections were fixed in 4% paraformaldehyde in 0.1 M PBS (pH 7.4) for 15 min, rinsed with 4× standard saline citrate (SSC; pH 7.4) and dehydrated using a graded ethanol series. The sections were

then hybridized overnight at 41 °C with the ^{35}S-labeled antisense or sense probe at 1.0×10^7 cpm/mL in hybridization buffer (50% formamide, 1% Denhardt's solution, 250 μg/mL tRNA, 0.1 g/mL dextran sulfate, 0.12 M PB, 0.02 mM/mL DTT in 4× SSC). After hybridization, the sections were rinsed three times with 1× SSC at 55 °C for 20 min, dehydrated using a graded ethanol series, coated with NBT2 emulsion (Eastman Kodak Company, Rochester, NY, USA) and exposed for 3 weeks at 4 °C. Finally, the sections were developed using a D-19 developer (Eastman Kodak) and observed under a light microscope (Figs. 7 and 8). The in situ hybridized hippocampal sections were counterstained with methyl green to visualize the nuclei (Fig. 9).
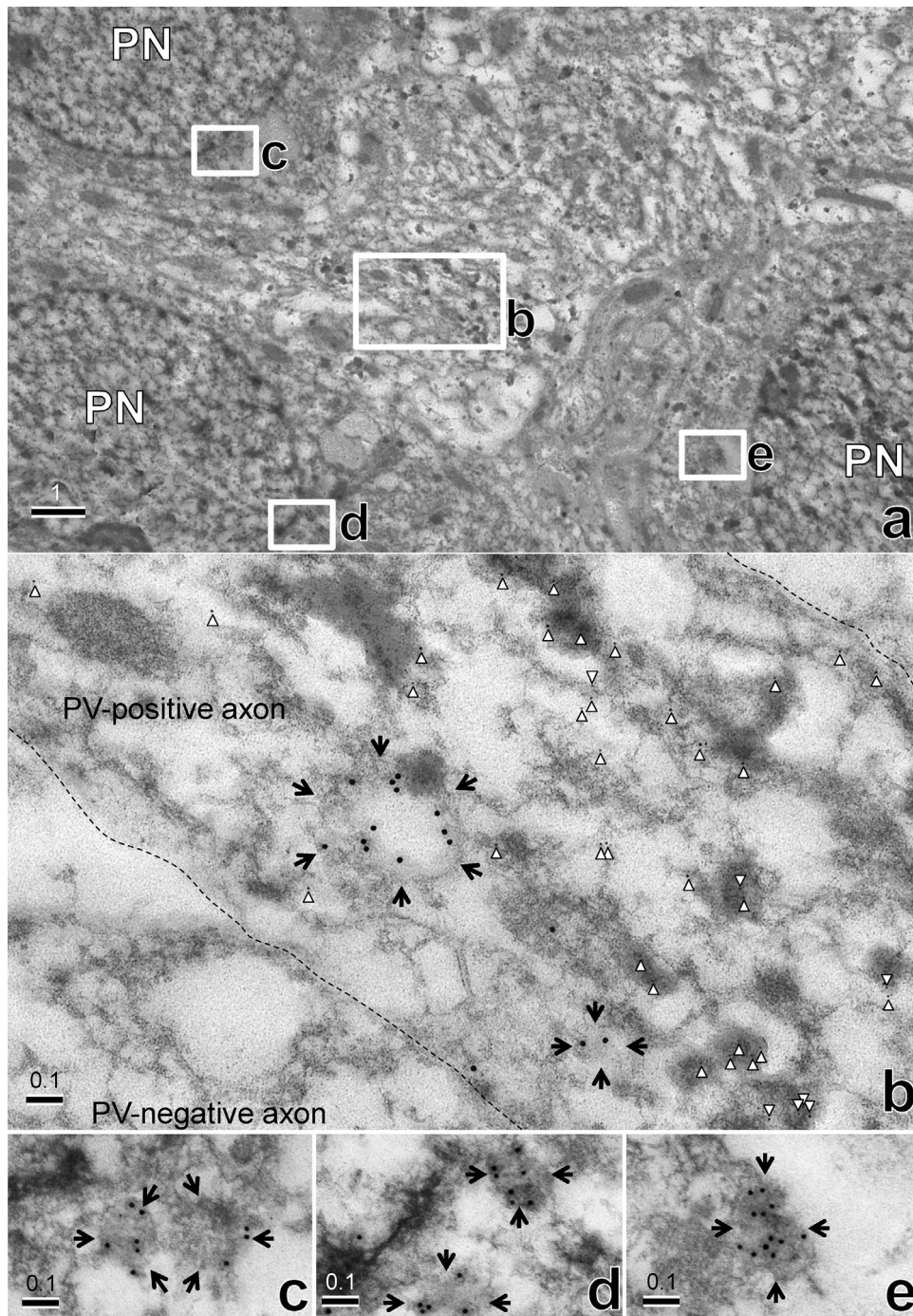
Fig. 6. Electron micrographs of pyramidal neurons and axons in the pyramidal layer of CA3 region with double-labeling of PS-IR (15 nm) with anti-saposin D antibody and PV-IR (5 nm) with anti-PV antibody. The PS-IR organelles seen in the rectangles in Fig. 6a are shown at higher magnification in Fig. 6b- e. PS-IR gold particles in three pyramidal neurons (PN) were observed in lysosome-like organelles (arrows in Fig. 6c-e). On the other hand, PS-IR gold particles in the PV-IR axon were observed in the pale vesicles (arrows in Fig. 6b), not resembling lysosome. PS like immunoreactivity (15 nm gold particles) stained with anti-saposin D antibody was observed in lysosome-like organelles (arrows) in the PV-positive (arrowheads) axon. The dotted lines express the borderlines of the PV-positive axon. Bars: The numbers on the bar indicate μm.

2.8. Statistical analysis

The relative intensities of immunoreactivity in the immunoblot bands (Fig. 1) or immunohistochemistry (Fig. 5) and hybridization signals (Fig. 10) in the hippocampus were blindly examined using computer-assisted image analysis. Briefly, digital images of the immunoblot bands and the central parts of CA1, CA3 and dentate gyrus (DG) were obtained using a Nikon A1 confocal microscope. The images were obtained under the same magnification and volt-age in order to stabilize brightness. The average gray value of all pixels in each image (Figs. 1a, c, 5c, f, i, l, o, r, 10a–e) was determined using NIH 1.56 software (public domain software by Dr. Steve Barrett). Then the ratio of the gray values obtained from the image was calculated. The statistical significance of the ratios was examined by one-way analysis of variance (ANOVA) and *post hoc* Fisher's PLSD tests using the program StatView (Abacus Concepts Inc., Berkeley, CA, USA).
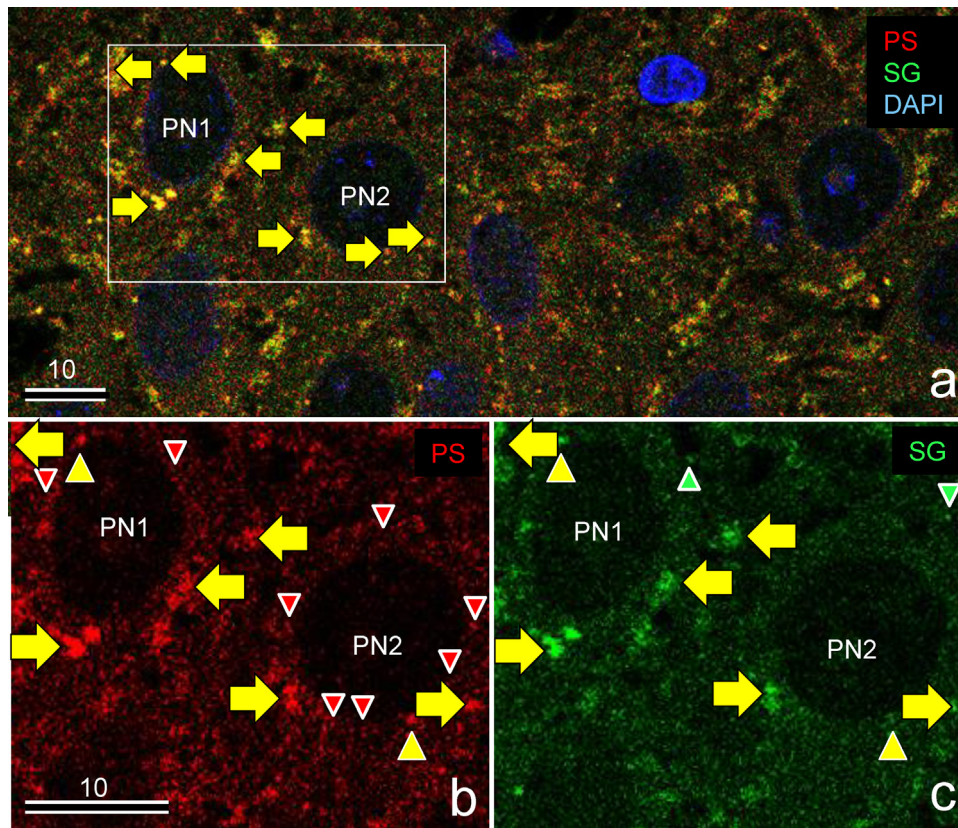
Fig. 7. Double immunofluorescence light micrographs of the CA3 regions of rats 3 days after KA injection stained with anti-PS (red), anti-segretogranin (SG:green) and DAPI (blue). Many dot-like structures around pyramidal neurons were double-stained with PS and SG (yellow arrows). Some small dot-like structures in the neurons were also double-stained with PS and SG (yellow arrowheads) in the neuronal cytoplasm. Small dot-like structures stained only with PS were indicated with red arrowheads mainly in the cytoplasm (Fig. 7b) and those stained only with SG were indicated with green arrowheads (Fig. 7c). The numbers on the bar indicate μm.

3. Results

3.1. Western blotting (Fig. 1)

Immunoblotting of the hippocampus using antibody against PS showed only one band at approximately 69 kDa and a clear increase in PS after KA injection (Fig. 1a, b), but there was no saposin band that was reported in the spleen and other tissues (Sano et al., 1989; Shimokawa et al., 2013).

Immunoblotting of the hippocampus using antibodies against PV showed a clear decrease after KA injection (Fig. 1c, d). This decrease in PV indicates the exhaustion of PV after KA injection.

Immunofluorescence staining of PS and GAD (Fig. 2)

To clarify which types of cells strongly express PS after KA injection, the colocalization of PS and GAD was examined by double immunostaining of the hippocampus 3 days after KA injection. The intensities of PS and GAD immunoreactivity (IR) in the interneurons increased, and were more intense overall than in the CA1 Pyramidal neurons (Fig. 2a, b). Besides the cell bodies of interneurons, PS and GAD double-IR axon terminals around pyramidal neurons were observed, and they were more numerous after the injection of KA (Fig. 2b) than PBS (Fig. 2a).

3.2. Change of GAD, PV, CB, CR immunoreactivity after KA injection (Fig. 3)

To determine which types of subpopulation of GABAergi neuron strongly express PS after KA injection, the colocalization of PS and GAD, PV, CB or CR was examined by double immunofluorescence staining of the hippocampus 3 days after KA injection (Fig. 3). The intensity of PS-IR in the PV positive interneuron was the strongest in these GABAergic markers (Fig. 3c), especially in the PV positive axonal terminals around the pyramidal neurons were extremely strong (Fig. 3d) compared with CB (Fig. 3f) and CR (Fig. 3h).

3.3. Change of PS and PV immunoreactivity after KA injection (Figs. 4 and 5)

In low-power micrographs of the hippocampus, the number of PV-positive neurons decreased after KA injection compared with PBS injection (Fig. 4, a and b). However, the intensity of PS-IR in axons around pyramidal neurons was much higher after KA injection than PBS injection in all areas. In particular, the number of PS and PV double positive axon terminals around the CA1 and CA3 pyramidal neurons was much higher after KA injection (Fig. 4, f and j) than PBS injection (Fig. 4, d and h). With the exception of the basal portion of the molecular layer, the number of PS and PV double positive axon terminals around DG granular neurons was low (Fig. 4, k and l). The diameter of PS-positive immunofluorescent reactions was 0.3–1.0 μm (Fig. 5, c, f, i, and l).

For morphometrical analysis of the difference in axonal PS-IR between KA and PBS injection, the red fluorescence of PS-IR (Fig. 5b, e, h, k, n, q) was changed to a black-and-white image (Fig. 5c, f, I, l, o, r), and the intensity was analyzed using NIH 1.56 software (public domain software by Dr. Steve Barrett)(Fig. 5s, t, u). The PS-IR in the axons around the CA1 and CA3 pyramidal neurons were significantly increased after KA injection compared with PBS injection (Fig. 5s, t), but PS-IR in the axons around the granular neurons in the DG increased moderately (Fig. 5u). Compared with CA1, a greater increase in PS-IR was observed in CA3 (Figs. 4a–h, 5).
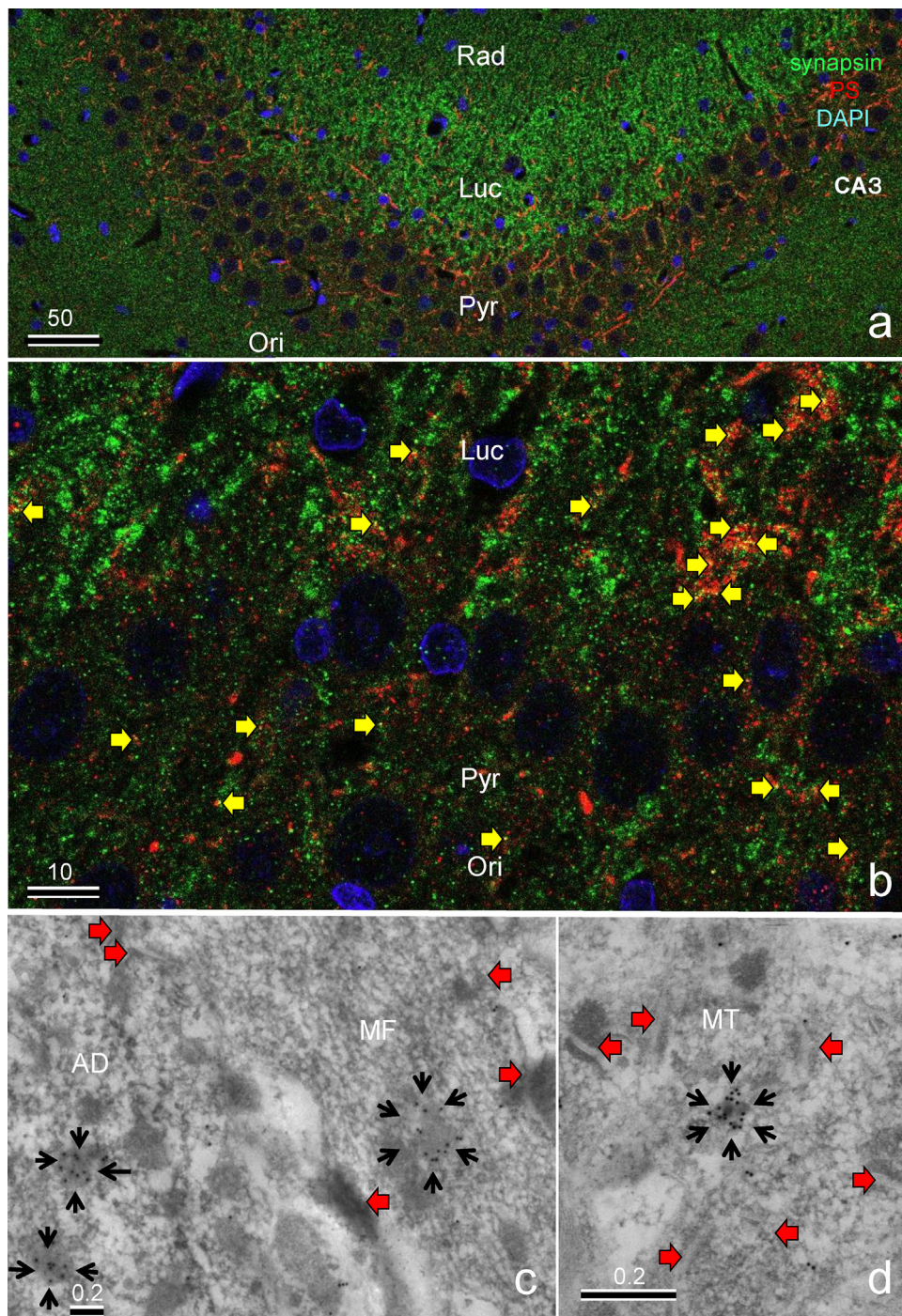
Fig. 8. **(a, b)** I(a, b) Immunofluorescence light micrographs of rat CA3 regions 1 day after KA injection stained with anti-PS, anti-synapsin II, and DAPI. The PS immunostaining (red) is very strong in the strata pyramidale (Pyr) and lucidum (Luc), and synapsin II (green) is distributed in all areas, being particularly strong in the stratum lucidum (a). Many dot-like structures around pyramidal neurons in the strata pyramidale and lucidum were stained by both PS and synapsin II (yellow arrows in b) **(c, d)** Electron micrographs of the stratum lucidum in the CA3 region with double-labeling of PS-IR (15 nm) with anti-saposin D antibody and PV-IR (5 nm). In these micrographs, no PV-IR was observed. (c) PS-IR gold particles in lysosome-like organelles (arrows) were observed in the apical dendrite (AD) of pyramidal neurons and mossy fibers (MF) with many desomosome-like structures (red arrows), synaptic vesicles, and bundles of microtubules and neurofilaments. (d) PS-IR gold particles densely packed in small lysosome-like structures (arrows) were observed in the mossy terminal (MT) with many desomosome-like structures (red arrows). The numbers on the bar indicate μm..

3.4. PS immunoreactivity in the PV positive axon terminals with electron microscopy (Figs. 6 and 8)

Electron micrographs of the pyramidal layer of CA3 region stained with anti-saposin D and anti-PV showed that saposin D-IR gold particles in the pyramidal neurons (PN) were localized in lysosome-like organelles (arrows in Fig. 6c–e) as reported before (Hosoda et al., 2007). On the other hand, saposin D –IR gold particles in the PV-IR axon were observed in the pale vesicles (arrows in Fig. 6b), not resembling lysosome. The diameter of these saposin D –IR vesicles was about 0.1–0.4 μm
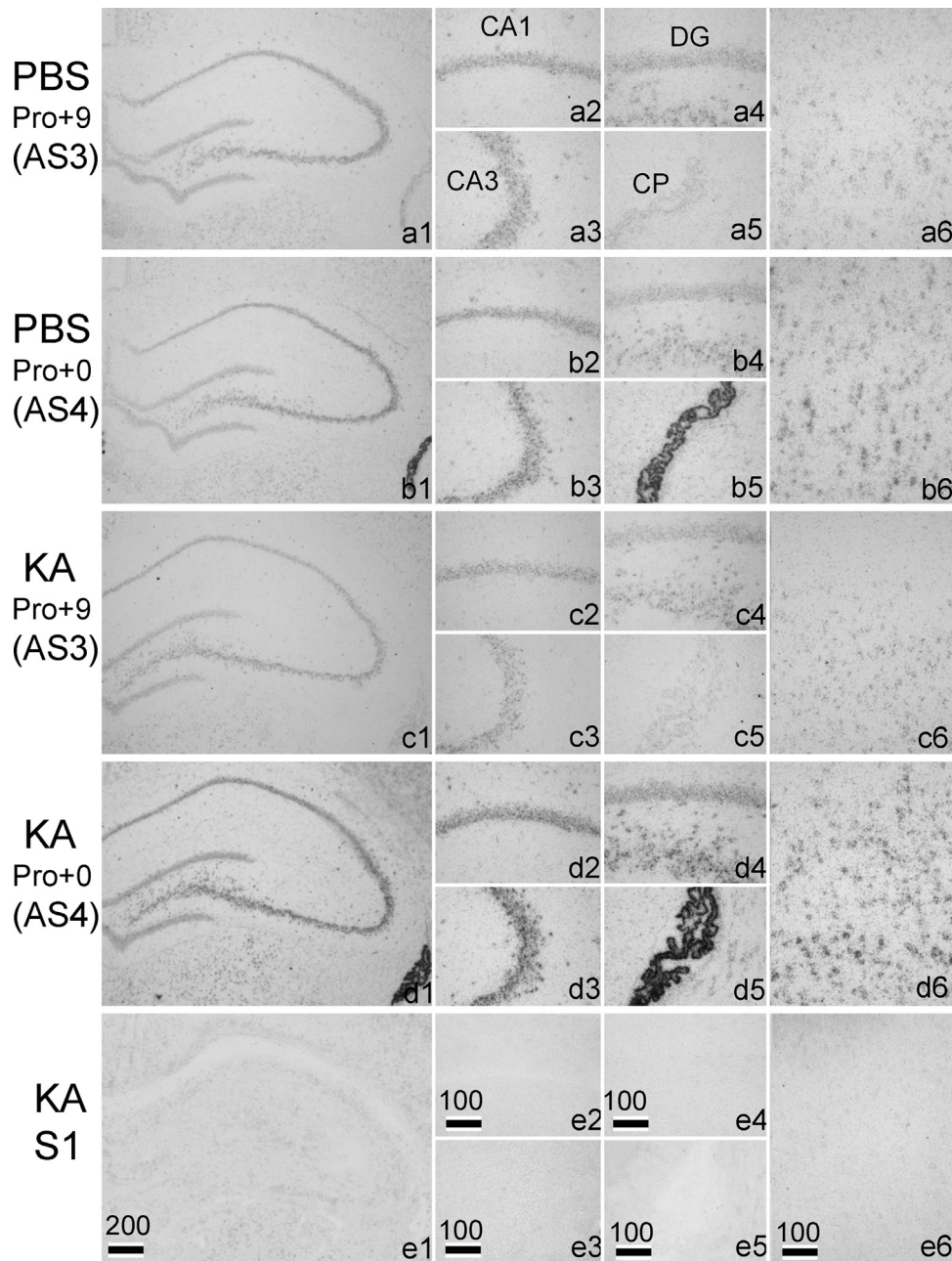
Fig. 9. *In situ* hybridization of the hippocampus showing PS mRNA in the rats 3 days after PBS injection (a, b) or KA injection (c, d, e). PS mRNA expression increased after KA injection compared with PBS injection in all areas. Pro + 0 is more intense than Pro + 9 both in KA and PBS injection. The numbers on the bar indicate μm.

3.5. PS immunoreactivity colocarized with segretogranin (SG) or synapsin (SS) (Fig. 7 and 8)

Double immunofluorescence light micrographs with anti-PS, anti-SG and DAPI showed that many dot-like structures around pyramidal neurons were double-stained with PS and SG (Fig. 7). Some small dot-like structures double-stained with PS and SG were also observed in the neuronal cytoplasm. Small dot-like structures stained only with PS were observed mainly in the cytoplasm (Fig. 7b) and those single-stained with SG were also observed (Fig. 7c).

Double immunofluorescence light micrographs of the CA3 regions of the animal 1 day after PBS injection stained with anti-PS, anti-synapsin II and DAPI showed that many dot-like structures around pyramidal neurons were double-stained with PS and synapsin II (Fig. 8). The immunostaining of PS is strong in the strata pyramidale and lucidum, and that of synapsin II is very strong in stratum lucidum (Fig. 8a). Many dot-like structures around pyramidal neurons in the strata pyramidale and lucidum were stained both with PS and synapsin II (Fig. 8b).

Electron micrographs of the stratum lucidum in the CA3 region, in the same section as in Fig. 6, showed PS-IR gold particles in lysosome-like organelles in the apical dendrites of pyramidal neurons and mossy fibers (Fig. 8c). PS-IR gold particles densely packed in small lysosome-like structures were observed in the mossy terminal with many desomosome-like structures (Fig. 8d).

3.6. Expression of PS mRNA after KA injection (Figs. 9–11)

In situ hybridization was performed in the adult rat brain with the following probes: PS-AS4 for Pro + 0 mRNA, PS-AS3 for Pro + 9 mRNA, PS-AS1 for both Pro + 0 and Pro + 9 mRNAs and the sense
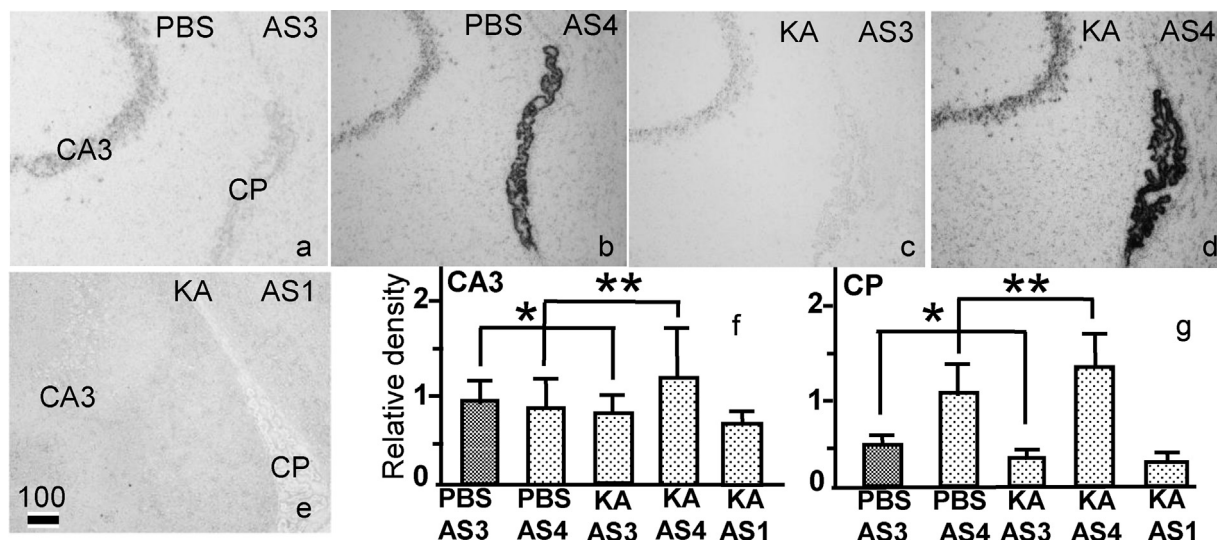
Fig. 10. Comparison of PS mRNA signals in the hippocampal CA3 and choroid plexus (CP) in rats 3 days after KA or PBS injection. Relative density of AS4 (Pro + 0) PS mRNA, semi-quantified using NIH Image software, with background intensity subtracted, significantly increased both in CA3 and CP after KA injection compared with the PBS-injected control (n = 6); intensities are presented as means ± standard error (S.E.) (*P < 0.05, **P < 0.01). The numbers on the bar indicate μm.

probe PS-S1 for the sequence complementary to PS-AS1 (Hosoda et al., 2007; Chen et al., 2008; Xue et al., 2011; Li et al., 2013; Shimokawa et al., 2013; Saito et al., 2014).

In the PBS-injected control animals, weak hybridization signals of PS-AS3 (Pro + 9) were observed in the neuronal cell layers of hippocampal CA1, CA2, CA3, CA4, DG, choroid plexus and cerebral cortex (Fig. 9a1-6). Similar hybridization signals of PS-AS4 (Pro + 0) were observed in the neuronal cell layers of hippocampal CA1, CA2, CA3, CA4, DG and cerebral cortex (Fig. 9b1-4, b6), except for the choroid plexus where strong signals were observed (Fig. 9b5).

In the KA-injected animals, weak hybridization signals of PS-AS3 (Pro + 9) were similar in all areas of the PBS-injected animals (Fig. 9c1-6). In contrast, strong hybridization signals of PS-AS4 (Pro + 0) were observed in the neuronal cells of all areas (Fig. 9d1-4, b6), and very strong signals were observed in the choroid plexus (Fig. 9d5). The control sections stained with sense oligonucleotide probe (PS-S1) showed only faint hybridization signals in all areas (Fig. 9e1-6).

morphometrical analysis of the difference in hybridization signals (Fig. 10)

For morphometrical analysis of the difference in hybridization signals between PS-AS3, PS-AS4, PS-S1 after KA or PBS injection, the photomicrographs were taken in the same condition of microscope illumination (Fig. 10a-e), and their intensities were analyzed using NIH 1.56 software (Fig. 10f). The hybridization signals of PS-AS4 in the all areas and choroid plexus were significantly increased after KA injection compared with PBS injection (Fig. 10f, g).

3.7. Expression of PS mRNA observed in the higher magnification after nuclear counterstaining (Fig. 11)

The sections of *in situ* hybridization were counterstained with methyl green to visualize the nuclei as well as the hybridization signals (Fig. 11). The signals of AS4 were much stronger than those of AS3 in the all areas of the hippocampus, cerebral cortex and choroid plexus (Fig. 11), especially in the CA3 (Fig. 11d) and the choroid plexus (Fig. 11l).

In the higher magnification, the signals of each cell show a wide variety of intensity in the CA3 (Fig. 11c, d), CA4 (Fig. 11e, f), and the cerebral cortex (Fig. 11e, f), but rather even in the CA1 (Fig. 11a, b) and DG (Fig. 11g, h). The strong signals in the CA3 region were localized mainly in the pyramidal layer, but some strong signals

were observed outside of the pyramidal layer, such as in the strata radiatum and lacunosum-moleculare or the upper portion of the stratum oriens (Fig. 11d). Based on their localization, size and form of nuclei, these cells appeared to be interneurons and not glial cells. These cells were observed mainly in the CA3 area (Fig. 10c, d), but a few in the CA1 area (Fig. 11a, b).

4. Discussion

In our previous study, we found the increase of PS mRNA level in the rat hippocampus and the choroid plexus after KA-induced brain injury, leading the notion that increased PS may contribute the prevention of apoptosis in the damaged neurons (Nabeka et al., 2014). In fact, a synthetic peptide corresponding to the neurotrophic activity region of PS prevented the KA-induced neurodegeneration (Nabeka et al., 2015). The increase of PS expression level also has been reported in the CNS after the sciatic nerve injury (Gillen et al., 1995), the transient forebrain ischemia (Yokota et al., 2001; Hiraiwa et al., 2003), the cortical stab wound injury (Hiraiwa et al., 2003), and the facial nerve transection (Chen et al., 2008). These studies indicate PS plays an important role in the healing process of the injured nervous system. In the present study, the higher increase of PS in CA3 compared with CA1 is most likely because the concentration of KA receptors is highest in CA3 (Malva et al., 1998; Wang et al., 2005).

Several alternatively spliced mRNAs are found for PS gene (Hiraiwa et al., 2003). Main two forms of them are the mRNA with or without 9-base insertion (Pro + 9 and Pro + 0 mRNA). Hiraiwa et al. (2003) reported that the expression ratio of Pro + 9 and Pro + 0 mRNA changes from 85:15 to 5:95 in the rat brain after experimental brain ischemia or cortical stab wound injury. Chen et al. (2008) also showed significant increase of Pro + 0 mRNA expression in the facial nerve nucleus after the facial nerve transection. In the present study, significant increase of Pro + 0 mRNA expression also has been observed not only in the pyramidal excitatory neuron but also in the inhibitory interneuron in the rat hippocampus after KA injection. These findings may indicate the transcript of Pro + 0 mRNA assumes the neurotrophic function in the healing process of the injured nervous system.

On the other hand, Pro + 9 mRNA is reportedly expressed preferentially in tissues in which the intact form of PS dominates, whereas Pro + 0 mRNA is preferentially expressed in tissues in which the
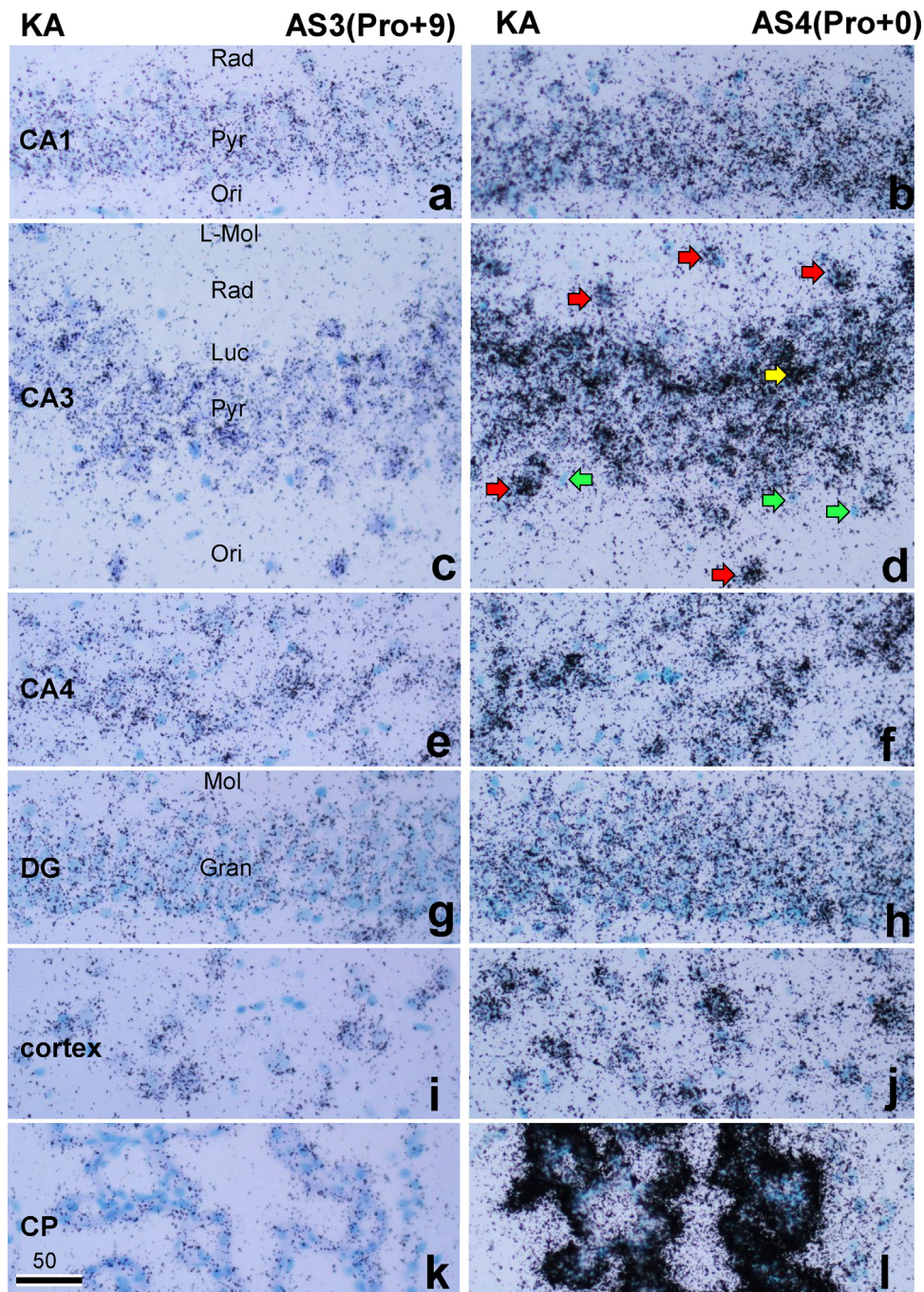
Fig. 11. *In situ* hybridization of the hippocampus showing PS mRNA expression at higher magnification. The hybridization signals are shown as tiny black dots, and the nuclei were stained bluish green with methyl green. The section stained with probe Pro + 9 showed only faint hybridization signals (left column), but the Pro + 0 signals (right column) in all hippocampal areas and choroid plexus (CP) were very intense. Red arrows indicate the intense interneurons in the extra-Pyr layer in CA3 region (d), yellow arrow indicates the interneuron in the intra-Pyr layer with slender nuclei, and green arrows indicate smaller glial nuclei without signal. The numbers on the bar indicates μm.

precursor dominates. Because the choroid plexus is responsible for the generation of cerebrospinal fluid containing the intact form of PS, the increase of Pro + 9 mRNA should be expected. But actually, clear increase in the neurons and choroid plexus after KA injection was Pro + 0 mRNA (Fig. 9d). Also in the previous study, we suggested that Pro + 0 mRNA is related to the intact form in the choroid plexus, and that the alternatively spliced forms of mRNAs do not simply correspond to the precursor and intact forms of PS (Saito et al., 2013).

Although the neurotrophic activity region was found in saposin C domain of PS, the alternative splicing occurred in its saposin B

domain (Holtschmidt et al., 1991a, 1991b). At present it is unclear for the neurotrophic function of the splicing region in injured nervous system. Interestingly, the choroid plexus generates the cerebrospinal fluid containing considerable amount of intact form PS (Hineno et al., 1991), and expresses Pro + 0 mRNA intensely but Pro + 9 mRNA weakly (Saito et al., 2014). In addition, the expression of Pro + 0 mRNA was found to increase in the choroid plexus on KA-induced brain injury in this study. Therefore, there is a possibility that Pro + 0 mRNA expression is convenient for synthesis and secretion of intact form PS in the nervous system. The increase of Pro + 0 mRNA in the inhibitory interneuron after KA injection and
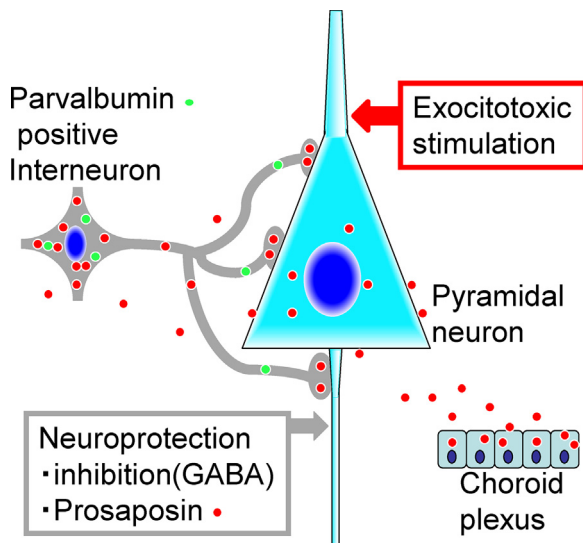
Fig. 12. Schematic presentation of the neuroprotection against exocitotoxic stimulation. The pyramidal neurons can produce neuroprotective PS and use it paracrine or autocrine manner. Parvalbumin (PV) positive interneurons around pyramidal layer can produce PS, transport it to the axon terminals and secrete it with GABA around the pyramidal neurons. The choroid plexus also produce and secrete PS to the cerebrospinal fluid react to the exocitotoxic stimulation of kainic acid.

PS-containing vesicles in the axon terminals of the interneuron, and the report that the interneuron may promote the survival of the pyramidal neuron by secreting the inhibitory neurotransmitter (Liang et al., 2009) lead us notion that PS is also one of the secreting factor from the interneuron around the pyramidal neuron for their survival in the injured hippocampus (Fig. 12).

In the present study, we also aimed to clarify which interneuron was up-regulated to produce PS and how PS function after systemic KA injection. Freund and Buzsáki (1996) proposed that the term hippocampal "interneuron" should be synonymous with "GABAergic with no principal cell". In the present study, interneurons outside of the pyramidal layer were easily defined, and those inside the pyramidal layer were defined as slender cell bodies and nuclei (Fig. 11d). Our previous results showed that PS mRNA signals in the interneurons increased abruptly 1 day after KA injection, and those of PS-IR increased after 1 day and peaked 3 days after KA injection (Nabeka et al., 2014). These results indicate that KA injection stimulated the interneurons to produce PS more strongly than the pyramidal neurons.

PV-positive interneurons account for approximately half of the GABAergic neurons in the hippocampus. Axon terminals fields immunoreactive for PV are extremely dense in the cell body layers and proximal stratum oriens. The majority of PV-positive varicosities surround the cell bodies and axon initial segments of principal neurons. This characteristic laminar distribution of PV-positive axon terminal fields overlaps with that of basket and axo-axonic (chandelier) neurons, suggesting that these morphologically identified neuron types selectively contain PV (Freund and Buzsáki, 1996). In a recent in-vivo study, intracellularly recorded and labeled basket neurons were shown to be immunoreactive for PV but not for CB or CR (Sík et al., 1995). In the present study, the majority of PV-positive bouton-like structures contain PS-IR (Figs. 4 and 5).

The increase in PV-IR in the axon seems to contradict with the results in Fig. 1, which shows a significant reduction in the level of PV protein (Fig. 1, c and e). However, the number of PV-IR neurons in the hippocampus decreased (Fig. 4, a and b). This reduction in PV-positive neurons may have caused the reduction of total PV content in the hippocampus. Decreased PV expression was also reported in PV-positive GABAergic interneurons in schizophrenia (Hashimoto

et al., 2003; Nakazawa et al., 2012). PV reduction may be related to some pathological states. A reduction in PV in neuronal cell bodies and an increase in PV in axons may indicate the movement of PV from neuronal bodies to axons in pathological conditions.

Liang et al. (2009) reported that the amplitudes of evoked inhibitory postsynaptic currents were increased significantly 12 h after ischemia and then returned to control levels 24 h following reperfusion with voltage clamp recording. They suggested that this transient enhancement of inhibitory neurotransmission might temporarily protect CA1 pyramidal neurons and delay neuronal death after cerebral ischemia. Therefore, transient enhancement of inhibitory neurons might protect pyramidal neurons by inhibitory currents (Fig. 12). Similarly, PS released from the axonal terminals of interneurons around the pyramidal neurons also might protect the pyramidal neurons (Fig. 12). Accordingly, the PS-IR in the bouton-like structures around the pyramidal neurons was strongly increased after KA injection (Fig. 5j-l).

PS mRNA expression in the choroid plexus of normal control animals was strong (Fig. 8b5), as reported previously (Saito et al., 2014). This observation is reinforced by the report that cerebrospinal fluid in normal animals contains a significant amount of PS (Hineno et al., 1991). Furthermore, 3 days after KA injection, the hybridization signal in the choroid plexus was very strong (Fig. 9d5). These results indicate that a lot of PS is produced in the choroid plexus and secreted into the cerebrospinal fluid after some direct or indirect KA stimulations to the choroid plexus (Fig. 12).

In conclusion, as Fig. 12 indicates, PV-positive inhibitory interneurons are the main neurons helping the pyramidal neurons from the exocitotoxic stimulation of kainic acid or other similar phenomenon caused by ischemia. Pyramidal neurons receive synaptic input, delivering inhibitory neurotransmitter (GABA) and neurotrofic factor (PS) that sustain neuronal survival (Fig. 12).

Neurotrophins, a family of secretory neurotrophic factors including NGF, BDNF, NT-3, NT-4/5, are famous to promote neuronal survival and differentiation. PS is also identified as a neurotrophins (O'Brien et al.,1994; Sorice et al., 2008). Neurotrophins, particularly BDNF, could elicit rapid and acute regulation of synaptic transmission and plasticity in the central nervous system (Lou et al., 2005). BDNF, NT-3 and PS have been reported to rerate with sortilin that controls intracellular sorting of BDNF (Chen et al., 2005) and PS (Yuan and Morales, 2011) to the regulated secretory pathway. Activity-dependent secretion of BDNF has been reported in many neuronal populations (See Lou et al., 2005), and its physiological significance has been highlighted by a number of recent studies (Chen et al., 2004; Egan et al., 2003). Taken together, it is not the infeasible idea that PS is also secreted in an activity-dependent manner especially after kainic acid neurotoxic stimulation.

Although, the mechanism of PS secretion is not clear, a possible mechanism of intracellular Ca^{2+}-dependent secretion is suggestive as the BDNF secretion reported in literature. Ca^{2+} influx through NMDA receptor/L-type VGCC and subsequent Ca^{2+} release of internal stores via ryanodine receptors are required for secretion. CaMKII, PKA, synaptotagmin IV, and CAPS2 also critically contribute to the membrane fusion process of BDNF-containing vesicles (Adachi et al., 2014). Further experiments about the change of these factors after kainic acid may clarify the mechanism of PS secretion.

Anti-PS IgG used in the present study was prepared to a synthetic oligopeptide corresponding to the proteolytic portion between saposin C and D, and reacts with PS but not with any of four saposins (Nabeka et al., 2014). The major proteolytic pathway of PS has been reported to begin with cleavage of saposin A from PS and progress from B-C-D trisaposin to B-C or C-D disaposins and finally to monosaposin (Qi and Grabowski, 2001). Our anti-PS IgG can react with B-C-D trisaposin, or C-D disaposin, but immunoblot analysis showed no band for these proteins (Fig. 1). Also in the

immunoblot of nervous tissues with anti-saposin D or anti-saposin B, the bands of trisaposin or disapsin were not observed but a faint band of saposin D was observed (Hosoda et al., 2007). These results indicate that PS works mainly with no or a few participation of proteolytic pathway in the nervous tissues.

Electron micrographs of the pyramidal layer of CA3 region stained with anti-saposin D and anti-PV showed PS-IR gold particles in the pale vesicles in the PV-IR axon. These vesicles were pale not resembling lysosome (Fig. 6b). On the other hand, the vesicles in the pyramidal neurons without PV-IR were dark, resembling ordinal lysosomes (Fig. 6c-e) as shown before (Hosoda et al., 2007). Unfortunately, as the specific antibody to PS could not react well with PS in the electron microscopy, we used anti-saposin D antibody that reacts both of PS and saposin-D. However, increased PS in PV positive axon-like structures was shown under a light microscope with specific antibodies to PS (Figs. 3–5). We believe that the gold particles in the pale vesicles in PV-IR axons are PS (Fig. 6b).

Secretogranins (SG) is a protein stored in secretory granules of endocrine cells (Rosa et al., 1985) and in large dense cored vesicles (LDCV) of neurons and neuroendocrine cells, and SG is thought to participate in the sorting and packaging of peptide hormones and neuropeptides into secretory granules (see Miyazaki et al., 2011). Miyazaki et al. (2011) showed that strong SG immunoreactivity was seen in PV-positive interneurons and nerve terminals, and suggested its role in the sorting and packaging of molecules other than neuropeptides in non-LDCV compartments. In the present study, SG was observed mainly in the putative axons or axonal terminal of interneurons around the pyramidal neurons in the hippocampal CA3 region (Fig. 7b, c), and SG thought to participate in the sorting and packaging of PS.

Recently, Meyer et al. (2013) identified GPR37 and GPR37L1, orphan G-protein-coupled receptors, as PS receptors. Following secretion, PS can undergo endocytosis via an interaction with the low-density lipoprotein- related receptor 1 (LRP1). The ability of secreted PS to promote protective effects in the nervous system is known to involve activation of G proteins, and the orphan G protein- coupled receptors GPR37 and GPR37L1 have recently been shown to mediate signaling induced by both PS and a fragment of PS known as prosaptide (see review of Meyer et al. 2014). Future studies should reveal whether a difference in the two saposin B isoforms of PS affects its affinity to these receptors.

Aknowlegements

References

Adachi, N., Numakawa, T., Richards, M., Nakajima, S., Kunugi, H., 2014. New insight in expression, transport, and secretion of brain-derived neurotrophic factor: Implications in brain-related diseases. World J. Biol. Chem. 5, 409–428.

Chen, J., Saito, S., Kobayashi, N., Sato, K., Terashita, T., Shimokawa, T., Mominoki, K., Miyawaki, K., Sano, A., Matsuda, S., 2008. Expression patterns in alternative splicing forms of prosaposin mRNA in the rat facial nerve nucleus after facial nerve transection. Neurosci. Res. 60, 82–94.

Chen, Z.Y., Patel, P.D., Sant, G., Meng, C.X., Teng, K.K., Hempstead, B.L., Lee, F.S., 2004. Variant brain-derived neurotrophic factor (BDNF) (Met66) alters the intracellular trafficking and activity-dependent secretion of wild-type BDNF in neurosecretory cells and cortical neurons. J. Neurosci. 24, 4401–4411.

Chen, Z.Y., Ieraci, A., Teng, H., Dall, H., Meng, C.X., Herrera, D.G., Nykjaer, A., Hempstead, B.L., Lee, F.S., 2005. Sortilin controls intracellular sorting of brain-derived neurotrophic factor to the regulated secretory pathway. J. Neurosci. 25, 6156–6166.

Collard, M.W., Sylvester, S.R., Tsuruta, J.K., Griswold, M.D., 1988. Biosynthesis and molecular cloning of sulfated glycoprotein 1 secreted by rat sertoli cells: sequence similarity with the 70-kilodalton precursor to sulfatide/GM1 activator. Biochemestry 27, 4557–4564.

Coyle, J.T., 1987. Kainic acid: insights into excitatory mechanisms causing selective neuronal degeneration. Ciba Found Symposium. 126, 186–203.

Dawson Jr., R., Beal, M.F., Bondy, S.C., Di Monte, D.A., Isom, G.E., 1995. Excitotoxins, aging, and environmental neurotoxins: implications for understanding human neurodegenerative diseases. Toxicol. Appl Pharmacol. 134, 1–17.

Egan, M.F., Kojima, M., Callicott, J.H., Goldberg, T.E., Kolachana, B.S., Bertolino, A., Zaitsev, E., Gold, B., Goldman, D., Dean, M., Lu, B., Weinberger, D.R., 2003. The BDNF val66met polymorphism affects activity-dependent secretion of BDNF and human memory and hippocampal function. Cell 112, 257–269.

Evans, S.F., Irmady, K., Ostrow, K., Kim, T., Nykjaer, A., Saftig, P., Blobel, C., Hempstead, B.L., 2011. Neuronal brain-derived neurotrophic factor is synthesized in excess, with levels regulated by sortilin-mediated trafficking and lysosomal degradation. J. Biological. Chem. 286, 29556–29567.

Ferkany, J.W., Zaczek, R., Coyle, J.T., 1982. Kainic acid stimulates excitatory amino acid neurotransmitter release at presynaptic receptors. Nature 298, 757–759.

Freund, T.F., Buzsáki, G., 1996. Interneurons of the hippocampus. Hippocampus 6, 347–470.

Gao, H.L., Li, C, Nabeka, H., Shimokawa, T., Saito, S., Wang, Z.Y., Cao, Y.M., Matsuda, S., 2013a. Attenuation of MPTP/MPP⁺ Toxicity in vivo and in vitro by an 18-mer Peptide Derived from Prosaposin. Neuroscience 236, 373–393.

Gao, H.L., Li, C, Nabeka, H., Shimokawa, T., Kobayashi, N., Saito, S., Wang, Z.Y., Cao, Y.M., Matsuda, S., 2013b. Decrease in prosaposin in the dystrophic mdx mouse brain. PLoS One 8, e80032.

Gao, H.L., Li, C, Nabeka, H., Shimokawa, T., Wang, Z.Y., Cao, Y.M., Matsuda, S., 2016. An 18-mer Peptide Derived from Prosaposin Ameliorates the Effect of Aβ1-42 Neurotoxicity on Hippocampal Neurogenesis and Memory Deficit in Mice. J. Alzheimer Dis. 53, 1173–1192.

Gillen, G., Gleichmann, M., Spreyer, P., Müller, H.W., 1995. Differentially expressed genes after peripheral nerve injury. J Neurosci Res 42, 159–171.

Hashimoto, T., Volk, D.W., Eggan, S.M., Mirnics, K., Pierri, J.N., Sun, Z., Sampson, A.R., Lewis, D.A., 2003. Gene expression deficits in a subclass of GABA neurons in the prefrontal cortex of subjects with schizophrenia. J. Neurosci. 23, 6315–6326.

Heggli, D.E., Aamodt, A., Malthe-Sørenssen, D., 1981. Kainic acid neurotxicity; effect of systemic injection on neurotransmitter markers in different brain regions. Brain Res. 230, 253–262.

Hineno, T.A., Sano, K., Kondoh, S., Ueno, Y., Kakimoto, K., Yoshida, K., 1991. Secretion of sphingolipid hydrolase activator precursor, prosaposin. Biochem. Biophys. Res. Commun. 176, 668–674.

Hiraiwa, M., Soeda, S., Kishimoto, Y., O'Brien, J.S., 1992. Binding and transport of gangliosides by prosaposin. Proc. Natl. Acad. Sci. U. S. A. 89, 11254–11258.

Hiraiwa, M., Liu, J., Lu, A.G., Wang, C.Y., Misasi, R., Yamauchi, I., Hozumi, I., Inuzuka, T., O'Brien, J.S., 2003. Regulation of gene expression in response to brain injury: enhanced expression and alternative splicing of rat prosaposin (SGP-1) mRNA in injured brain. J. Neurotrauma. 20, 755–765.

Holtschmidt, H., Sandhoff, K., Furst, W., Kwon, H.Y., Schnabel, D., Suzuki, K., 1991a. The organization of the gene for the human cerebroside sulfate activator protein. FEBS Lett. 280, 267–270.

Holtschmidt, H., Sandhoff, K., Kwon, H.Y., Harzer, K., Nakano, T., Suzuki, K., 1991b. Sulfatide activator protein. Alternative splicing that generates three mRNAs and a newly found mutation responsible for a clinical disease. J. Biol. Chem. 266, 7556–7560.

Hosoda, Y., Miyawaki, K., Saito, S., Chen, J., Bing, X., Terashita, T., Kobayashi, N., Araki, N., Shimokawa, T., Sano, A., Tanabe, H., Matsuda, S., 2007. Distribution of prosaposin in the rat nervous system. Cell Tissue Res. 330, 197–207.

Kishimoto, Y., Hiraiwa, M., O'Brien, J.S., 1992. Saposins: structure, function, distribution, and molecular genetics. J. Lipid Res. 33, 1255–1267.

Kondoh, K., Hineno, T., Sano, A., Kakimoto, Y., 1991. Isolation and characterization of prosaposin from human milk. Biochem. Biophys. Res. Commun. 181, 286–292.

Kondoh, K., Sano, A., Kakimoto, Y., Matsuda, S., Sakanaka, M., 1993. Distribution of prosaposin-like immunoreactivity in rat brain. J. Comp. Neurol. 334, 590–602.

Kotani, Y., Matsuda, S., Sakanaka, M., Kondoh, K., Ueno, S., Sano, A., 1996a. Prosaposin facilitates sciatic nerve regeneration in vivo. J. Neurochem. 66, 2019–2025.

Kotani, Y., Matsuda, S., Wen, T.-C., Sakanaka, M., Tanaka, J., Maeda, N., Kondoh, K., Ueno, S., Sano, A., 1996b. A hydrophilic peptide comprising 18 amino acid residues of the prosaposin sequence has neurotrophic activity in vitro and in vivo. J. Neurochem. 66, 2197–2200.

Lévesque, M., Avoli, M., 2013. The kainic acid model of temporal lobe epilepsy. Neurosci. Biobehav. Rev. 37, 2887–2899.

Li, C., Gao, H.L., Shimokawa, T., Nabeka, H., Hamada, F., Araki, H., Cao, Y.M., Kobayashi, N., Matsuda, S., 2013. Prosaposin expression in the regenerated muscles of mdx and cardiotoxin-treated mice. Histol. Histopathol. 28, 875–892.

Liang, R., Pang, Z.P., Deng, P., Xu, Z.C., 2009. Transient enhancement of inhibitory synaptic transmission in hippocampal CA1 pyramidal neurons after cerebral ischemia. Neurocience 160, 412–418.

Lothman, E.W., Collins, R.C., 1981. Kainic acid induced limbic seizures: metabolic, behavioral, electroencephalographic and neuropathological correlates. Brain Res. 218, 299–318.

Lou, H., Kim, S.K., Zaitsev, E., Snell, C.R., Lu, B., Loh, Y.P., 2005. Sorting and activity-dependent secretion of BDNF require interaction of a specific motif with the sorting receptor carboxypeptidase e. Neuron 45, 245–255.

Malva, J.O., Carvalho, A.P., Carvalho, C.M., 1998. Kainate receptors in hippocampal CA3 subregion: evidence for a role in regulating neurotransmitter release. Neurochem. Int. 32, 1–6.

Meyer, R.C., Giddens, M.M., Schaefer, S.A., Hall, R.A., 2013. GPR37 and GPR37L1 are receptors for the neuroprotective and glioprotective factors prosaptide and prosaposin. Proc. Natl. Acad. Sci. U. S. A. 110, 9529–9534.

Meyer, R.C., Giddens, M.M., Coleman, B.M., Hall, R.A., 2014. The protective role of prosaposin and its receptors in the nervous system. Brain Res. 1585, 1–12.

Miyazaki, T., Yamasaki, M., Uchigashima, M., Matsushima, A., Watanabe, M., 2011. Cellular expression and subcellular localization of secretogranin II in the mouse hippocampus and cerebellum. Eur. J. Neurosci. 33, 82–94.

Nabeka, H., Uematsu, K., Takechi, H., Shimokawa, T., Yamamiya, K., Chen, L., Doihara, T., Saito, S., Kobayashi, N., Matsuda, S., 2014. Prosaposin Overexpression following Kainic Acid-Induced Neurotoxicity. PLoS One 9, e110534.

Nabeka, H., Shimokawa, T., Doihara, T., Saito, S., Wakisaka, H., Hamada, F., Kobayashi, N., Matsuda, S., 2015. A Prosaposin-Derived Peptide Alleviates Kainic Acid-Induced Brain Injury. PLoS One 10, e0126856.

Nadler, J.V., Cuthbertson, G.J., 1980. Kainic acid neurotoxicity toward hippocampal formation: dependence on specific excitatory pathways. Brain Res. 195, 47–56.

Nadler, J.V., Evenson, D.A., Cuthbertson, G.J., 1981. Comparative toxicity of kainic acid and other acidic amino acids toward rat hippocampal neurons. Neuroscience 6, 2505–2517.

Nakazawa, K., Zsiros, V., Jiang, Z., Nakao, K., Kolata, S., Zhang, S., Belforte, J.E., 2012. GABAergic interneuron origin of schizophrenia pathophysiology. Neuropharmacology 62, 1574–1583.

O'Brien, J.S., Kretz, K.A., Dewji, N., Wenger, D.A., Esch, F., Fluharty, A.L., 1988. Coding of two sphingolipid activator proteins (SAP-1 and SAP-2) by same genetic locus. Science 241, 1098–1101.

O'Brien, J.S., Kishimoto, Y., 1991. Saposin proteins: structure, function, and role in human lysosomal storage disorders. FASEB J. 5, 301–308.

O'Brien, J.S., Carson, G.S., Seo, H.C., Hiraiwa, M., Kishimoto, Y., 1994. Identification of prosaposin as a neurotrophic factor. Proc. Natl. Acad. Sci. U. S. A. 91, 9539–9596.

Olney, J.W., de Gubareff, T., 1978. Glutamate neurotoxicity and Huntington's chorea. Nature 271, 557–559.

Qi, X., Grabowski, G.A., 2001. Molecular and cell biology of acid beta-glucosidase and prosaposin. Prog. Nucl. Acid Res. Mol. Biol. 66, 203–239.

Rosa, P., Fumagalli, G., Zanini, A., Huttner, W.B., 1985. The major tyrosine-sulfated protein of the bovine anterior pituitary is a secretory protein present in gonadotrophs, thyrotrophs, mammotrophs, and corticotrophs. J. Cell. Biol. 100, 928–937.

Sík, A., Penttonen, M., Ylinen, A., Buzáki, G., 1995. Hippocampal CA1 interneurons: an in vivo intracellular labeling study. J. Neuroci. 15, 6651–6665.

Saito, S., Saito, K., Nabeka, H., Shimokawa, T., Kobayashi, N., Matsuda, S., 2014. Differential expression of the alternatively spliced forms of prosaposin mRNAs in the rat choroid plexus. Cell Tissue Res. 356, 231–242.

Sano, A., Radin, N.S., Johnson, L.L., Tarr, G.E., 1988. The activator protein for glucosylceramide β-glucosidase from guinea pig liver. J. Biol. Chem. 263, 19597–19601.

Sano, A., Hineno, T., Mizuno, T., Kondoh, K., Ueno, S., Kakimoto, Y., Inui, K., 1989. Sphingolipid hydrolase activator proteins and their precursors. Biochem. Biophys. Res. Commun. 165, 1191–1197.

Sano, A., Mizuno, T., Kondoh, K., Hineno, T., Ueno, S., Kakimoto, Y., Morita, N., 1992. Saposin-C from bovine spleen: complete amino acid sequence and relation between the structure and its biological activity. Biochem. Biophys. Acta 1120, 75–80.

Sano, A., Matsuda, S., Wen, T.C., Kotani, Y., Kondoh, K., Ueno, S., Kakimoto, Y., Yoshimura, H., Sakanaka, M., 1994. Protection by prosaposin against ischemia-induced learning disability and neuronal loss. Biochem. Biophys. Res. Commun. 204, 994–1000.

Sato, K., Tohyama, M., 1998. Assessment of distribution of cloned ion channels in neuronal tissues. Methods Enzymol. 293, 155–165.

Schwob, J.E., Fuller, T., Price, J.L., Olney, J.W., 1980. Widespread patterns of neuronal damage following systemic or intracerebral injections of kainic acid: a histological study. Neuroscience 5, 991–1014.

Shimokawa, T., Nabeka, H., Yamamiya, K., Wakisaka, H., Takeuchi, T., Kobayashi, N., Matsuda, S., 2013. Distribution of prosaposin in rat lymphatic tissues. Cell Tissue Res. 352, 685–693.

Sorice, M., Molinari, S., Di Marzio, L., Mattei, V., Tasciotti, V., Ciarlo, L., Hiraiwa, M., Garofalo, T., Misasi, R., 2008. Neurotrophic signalling pathway triggered by prosaposin in PC12 cells occurs through lipid rafts. FEBS J. 275, 4903–4912.

Sun, A.Y., Chen, Y.M., 1998. Oxidative stress and neurodegenerative disorders. J. Biomed. Sci. 5, 401–414.

Terashita, T., Saito, S., Miyawaki, K., Hyodo, M., Kobayashi, Y., Shimokawa, T., Saito, K., Matsuda, S., Gyo, K., 2007. Localization of prosaposin in rat cochlea. Neurosci. Res. 57, 372–378.

Tsuboi, K., Hiraiwa, M., O'Brien, J.S., 1998. Prosaposin prevents programmed cell death of rat cerebellar granule neurons in culture. Brain Res. Dev. Brain Res. 110, 249–255.

Unuma, K., Chen, J., Saito, S., Kobayashi, N., Sato, K., Saito, K., Wakisaka, H., Mominoki, K., Sano, A., Matsuda, S., 2005. Changes in expression of prosaposin in the rat facial nerve nucleus after facial nerve transection. Neurosci. Res. 52, 220–227.

Wang, Q., Yu, S., Simonyi, A., Sun, G.Y., Sun, A.Y., 2005. Kainic acid-mediated excitotoxicity as a model for neurodegeneration. Mol. Neurobiol. 31, 3–16.

Xue, B., Chen, J., Gao, H., Saito, S., Kobayashi, N., Shimokawa, T., Nabeka, H., Sano, A., Matsuda, S., 2011. Chronological changes in prosaposin in the developing rat brain. Neurosci. Res. 71, 22–34.

Yokota, N., Uchijima, M., Nishizawa, S., Namba, H., Koide, Y., 2001. Identification of differentially expressed genes in rat hippocampus after transient global cerebral ischemia using subtractive cDNA cloning based on polymerase chain reaction. Stroke 32, 168–174.

Yuan, L., Morales, C.R., 2011. Prosaposin sorting is mediated by oligomerization. Exp. Cell Res. 317, 2456–2467.